Mini Review

Corrosion of General Oil-field Grade Steel in CO_2 Environment - an Update in the Light of Current Understanding

Mobbassar Hassan Sk, Aboubakr M Abdullah[*]

Center for Advanced Materials, CAM, Qatar University, Doha, 2713, Qatar
[*]E-mail: abubakr_2@yahoo.com , bakr@qu.edu.qa

In this review, we discussed the current mechanistic understanding and effects of key parameters on corrosion of carbon and low alloy steel (CLAS) in CO_2 environments. In particular, we emphasized on the current understanding related to the mechanism of early stage nucleation of siderite that has evolved from the outcomes of in-situ synchrotron-based X-ray studies under various modes. We also highlighted the effect of the most important environmental and metallurgical factors affecting the corrosion behavior of CLAS. Finally, we addressed the aspects of material chemistry and micro-alloying necessary for achieving the most effective and economic materials system for mitigating corrosion in CO_2 environment.

1. INTRODUCTION

Internal corrosion of oil-field grade steel components in aqueous CO_2 was first identified in 1940 and has been investigated over the last six decades [1-3]. Since then, CO_2 corrosion is well known to affect the integrity of carbon and low alloy steel [1-11]. It is considered as one of the most prevalent internal corrosion mechanisms associated with the oil production and refinery components (e.g. pipelines, down-hole units etc.) [1,7]. The cost of equipment failure due to CO_2 corrosion is significantly high [1, 12-17]. A survey conducted in 1970 indicated that ~ 28% of all oil-field related failures originated from CO_2 corrosion [18].

Most oil pipelines and oil-field equipment are built of plain carbon steel. Even though corrosion resistant alloys can be employed for mitigating the CO_2 corrosion, carbon steel is still the best choice in terms of economy and environmental friendliness. 95% of the constructional materials used in the oil and gas industries are carbon steel [12]. Efforts are continuing, with the objective of reducing the damage and cost associated with CO_2 corrosion and to extend the life of the oil-field

equipment. It is believed that slight modification of the chemical compositions of the plain carbon steels with desired elements at micro levels and engineering the surface characteristics could make carbon and low alloy steels (CLAS) inherently corrosion resistant.

Dry CO_2 is not corrosive within the normal operating temperatures range (< 150 °C) that oil and gas production components encounter. Nevertheless, CO_2 in water medium forms a weak acid which is capable of producing significant corrosion (up to several mm yr^{-1}). Depending on the exposure conditions, nature and protectivity of the scales vary significantly [1, 4, 19-28]. Furthermore, the morphology, chemistry, density and protectivity of the scales can be different for similar grade steels produced through different manufacturing process [29-31].

A major constituent of the CO_2 corrosion scale is ferrous carbonate ($FeCO_3$ or siderite). Generally, it provides protection against corrosion of carbon steel up to a certain extent under certain parametric conditions [1, 32]. Siderite scale is chemically stoichiometric and precipitates when the solubility product of Fe^{2+} and CO_3^{2-} cross the supersaturation limit. Nonetheless, mechanics of formation of siderite, especially at the early nucleation stage and its effect on the corrosion rate are still unclear. Various empirical and mechanistic models on the basis of laboratory findings as well as real field data are available to predict CO_2 corrosion rate for expected service conditions. These models are good means for controlling maintenance issues (e.g. interval projection), deciding about the proper steel of choice and requirement for chemical corrosion inhibition. In addition, there are predictive corrosion models which are used to determine the availability of required inhibitor, maximum allowable fluid velocities and inspection intervals [33-35]. However, one of the problems of relying on the available CO_2 corrosion prediction models is that these models often fail to include the effect of protective iron carbonate scaling into them or incorporate a relatively small effect of protective corrosion scales in its CO_2 corrosion prediction. Nyborg [21,36], in an overview of the prediction models, pointed out that these CO_2 corrosion prediction models differ substantially in terms of addressing the protective effect of the corrosion scale, to an extent that practically significant differences are often observed in the predicted corrosion rates.

Details of the formation mechanism of the corrosion scale and the factors that are critical in determining the protectiveness of such scale are debatable. Even though, conventional ex-situ experimentations revealed the corrosion scales are mainly $FeCO_3$, the morphology, composition and protectiveness of the scale are found to vary considerably e.g. [7, 37-39]. Also, under certain conditions (e.g. temperature > 80 °C and pH > 6), $FeCO_3$ forms a tightly packed and adherent crystalline scale which renders significant protection to the underlying steel. In addition to the presence of siderite, the presence of iron oxides/hydroxides is also identified in a few studies [e.g. 40], which however been considered as the artifacts of the ex-situ analysis. Oxides/hydroxides are presumed to be formed after the sample was removed from the de-oxygenated CO_2 environment [41].

Despite the importance of the formation of a protective surface scale of siderite in determining the overall corrosion rate of the steel, the majority of the works on CO_2 corrosion have been found to be focused on the mechanism and kinetics of the applicable cathodic reactions [42-44]. On the other hand, only a little information is available on the experimental as well as theoretical analysis of the anodic reactions that are directly related to the formation of carbonate scale. In addition, whatever little information was available about the early nucleation stages of scale formation, its mechanism and

subsequent growth are ambiguous. In the recent times, analysis of the experiments conducted in-situ, using synchrotron generated high flux X-ray in various modes e.g. X-ray diffraction, small angle X-ray scattering (SAXS), wide angle x-ray scattering (WAXS), grazing incidence small angle X-ray scattering (GISAXS), provided valuable information to formulate an effective understanding of the mechanism of the early stage nucleation and subsequent growth of the siderite crystal. These in-situ experimentation techniques have been very helpful as they facilitated monitoring the time-resolved growth of surface layers formed on a steel surface with changing electrochemical conditions which can be administered from outside [45, 49-54].

The purposes of this review are to address (i) the most updated understanding of the mechanism of CO_2 corrosion as a function of various exposure conditions, including the recent findings related to the early nucleation stage of siderite scale formation during CO_2 corrosion in CLASs revealed by in-situ synchrotron studies (ii) addressing the feasibility of using CLASs as the most effective oil-field grade steel in consideration of economy and durability.

2. CO₂ CORROSION SCALE – MODERN UNDERSTANDING DERIVED FROM IN-SITU SYNCHROTRON STUDY

CO_2 corrosion primarily manifests in the form of general corrosion and three variants of localized corrosion, namely pitting, mesa attack and flow-induced localized corrosion elaborated elsewhere [e.g. 7, 15].

Aqueous CO_2 corrosion of plain carbon steel is a reasonably well understood electrochemical process involving the anodic dissolution of iron and the cathodic evolution of hydrogen with an overall reaction -

$$Fe + CO_2 + H_2O => FeCO_3 + H_2 \quad\quad [1]$$

Solid ferrous carbonate ($FeCO_3$) forms as a precipitate according to

$$Fe^{2+} + CO_3^{2-} \Leftrightarrow FeCO_3 \text{ (s)} \quad\quad [2]$$
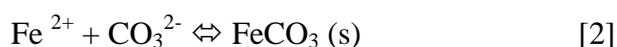
when the concentrations of Fe^{2+} and CO_3^{2-} ions exceed the solubility product limit. The precipitation process can be seen as the process of the solution returning to equilibrium and is driven by the magnitude of the supersaturation. The rate of the precipitation R_{FeCO_3} is therefore often expressed [3] as

$$R_{FeCO_3} = k_{e(FeCO_3)} \frac{A}{V} k_{sp(FeCO_3)}(SS_{(FeCO_3)} - 1) \quad [3]$$

where $k_{e(FeCO_3)}$ is a kinetic constant, which can be derived from the experimental results as a function of temperature, using an Arrhenius type equation

$$k_{e(FeCO_3)} = A_{FeCO_3} \exp\left(- \frac{B_{FeCO_3}}{RT_k}\right) \quad\quad [4]$$

where A_{FeCO_3} = 28.2 and B_{FeCO_3} = 64.851 J mol^{-1}

In practice ferrous and carbonate ions are frequently found in the aqueous solution at concentrations much higher than predicted by the equilibrium $k_{sp(FeCO_3)}$[4]. This is termed as supersaturation which is a necessary condition before any substantial precipitation can occur.

Details of the chemical, electrochemical, and transport processes involved in CO_2 corrosion of steel are elaborately described elsewhere [e.g. 4, 7].
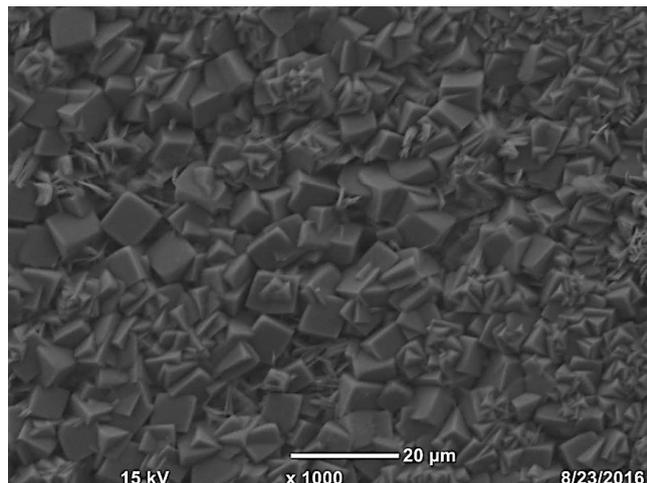

Figure 1. SEM of ferrous carbonate scale formed on plain carbon steel at $80^{o}C$, pH = 6.6, pCO_2 = 1 bar, stagnant conditions. This image is an outcome of our ongoing research activities.
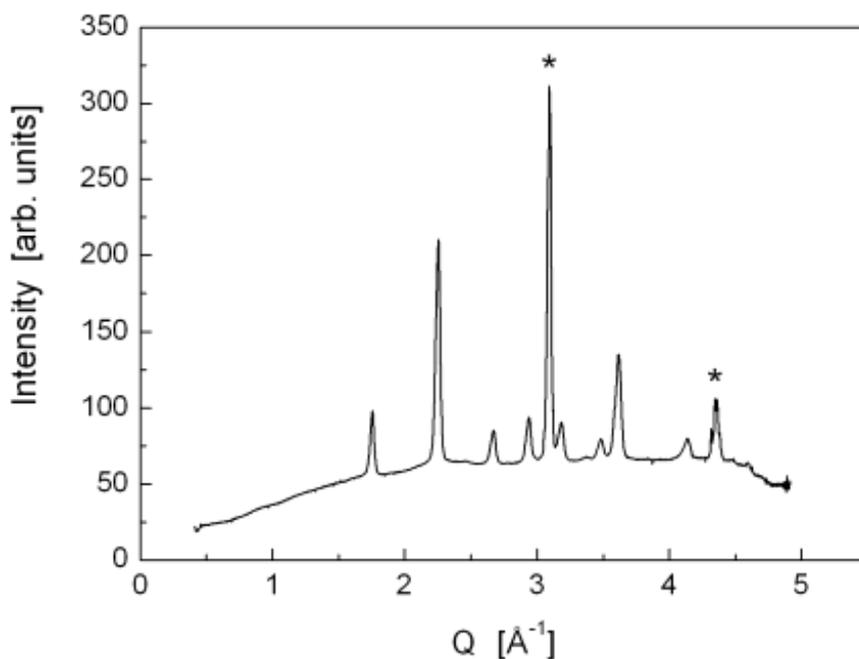
Figure 2. Ex-situ XRD results for the $FeCO_3$ surface scale formed in a potentiostatic test in the 0.5M NaCl solution at pH 6.3 and an applied potential of 500 mV (vs. Ag/AgCl, 3 M KCl). * indicates the substrate Fe [50]

Figure 1 illustrates SEM images of a crystalline ferrous carbonate layer formed on a plain carbon steel substrate after the ex-situ electrochemical test. The initially formed ferrous carbonate layer at the steel surface can act as a diffusion barrier for the species involved in the corrosion process. The

presence of scale at the steel surface thus changes the surface conditions and either makes the corrosion process stop or sluggish [4]. Figure 2 illustrates ex-situ XRD characteristics indicating the formation of siderite on carbon steel obtained during a potentiostatic test conducted in a CO_2 environment.
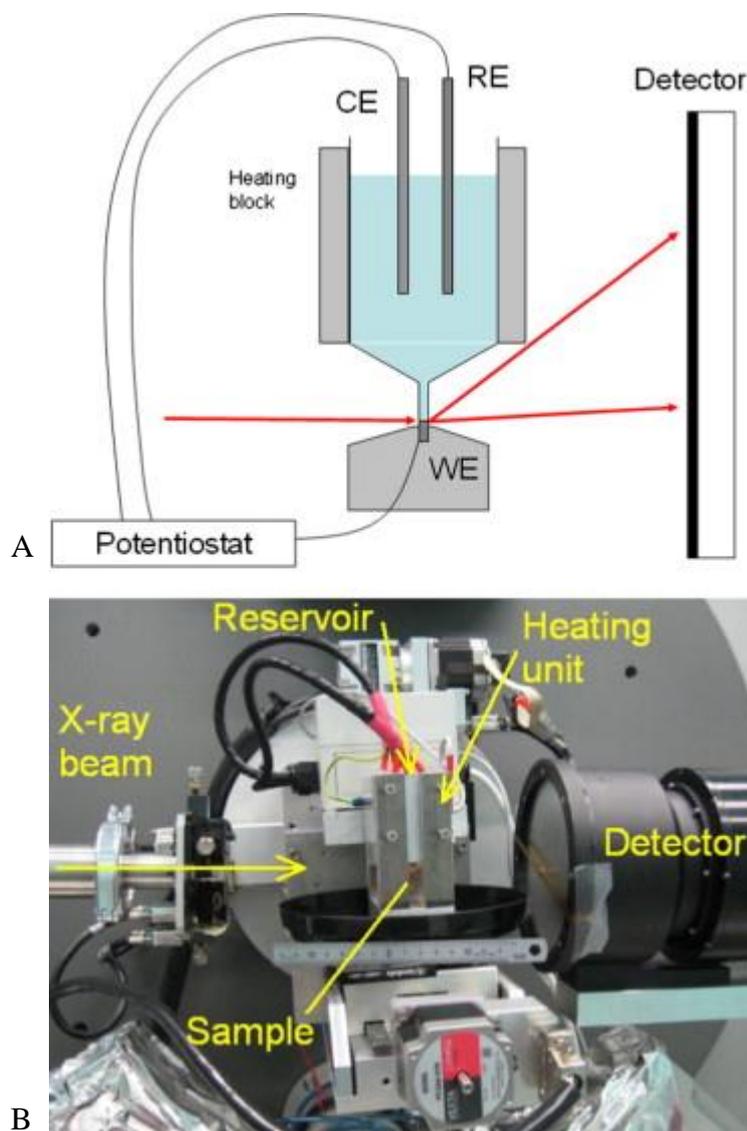
Figure 3. Diagram (a) and Photograph (b) of the cell as used on the Australian synchrotron powder diffraction beam line for *in situ* XRD experiments [45]

The effective protectiveness of a solid ferrous carbonate layer depends on its porosity, which is determined by the competition between the precipitation rate and the underlying corrosion rate. For precipitation rates higher than the corrosion rate, a dense and protective ferrous carbonate layer is expected, while a precipitation rate lower than the corrosion rates would lead to the formation of porous non-protective ferrous carbonate layers. By nature the protective layers are often found to be thin as they progressively reduce ionic transport and corrosion reaction, whereas non-protective layers are normally thick. [47, 48].

Despite the availability of the detailed knowledge about the chemical, electrochemical and transport processes associated with the formation of ferrous carbonate, information available about the mechanism of early nucleation stages of $FeCO_3$ (siderite) scale was only speculative. Nonetheless, current in-situ experimentation and investigation employing synchrotron-based high flux X-ray at various modes (XRD, SAXS, GISAX, WAXS) [45, 46, 49-52] shaded some light on the early stage nucleation of siderite scale during CO_2 corrosion of mild steel in brine environment. Figure 3(a) and (b) illustrate the schematic of experimental setup and photograph for in-situ synchrotron X-ray diffraction experiments using the powder diffraction Australian beam line. In-situ synchrotron X-ray diffraction technique made it possible to monitor the gradual real time development of the constituent phases of the corrosion scale with the changing electrochemical conditions that can be controlled from outside.
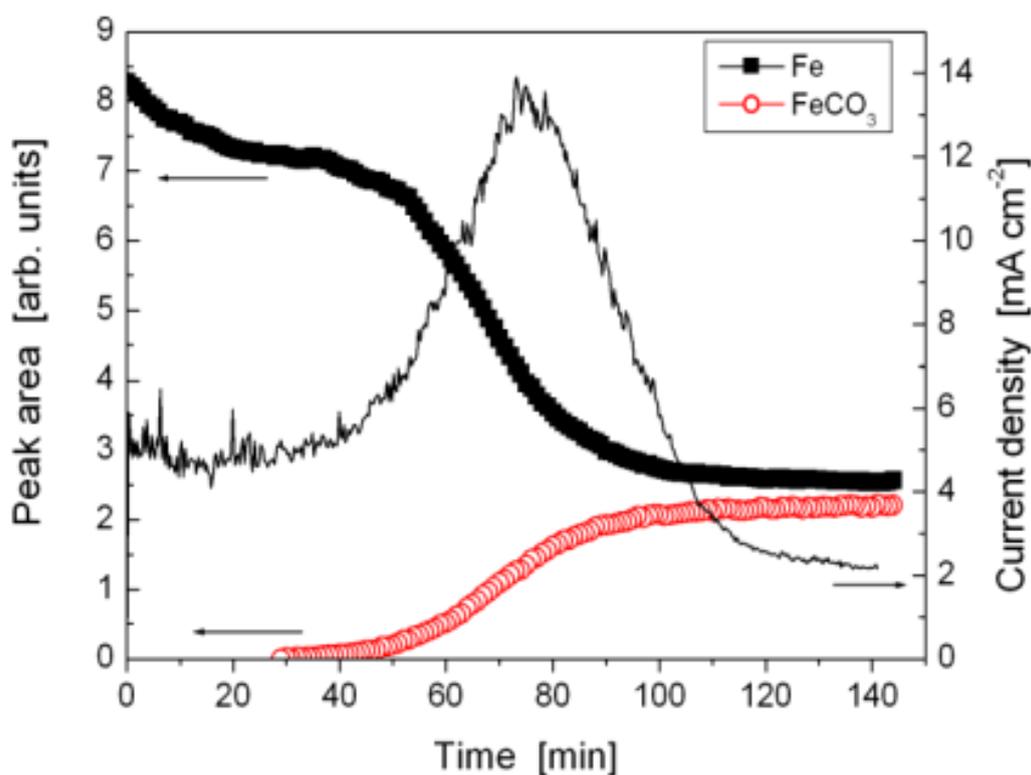
Figure 4. Results for 0.5 M NaCl solution, pH 6.3 and 80°C (applied potential of -500 mV) [45]

Figure 4 shows the anodic current as a function of time in a potentiostatic test in the NaCl solution at pH 6.3 (pCO_2 = 1bar) and an applied potential of -500 mV (*vs* SCE), together with the intensities of the Fe and $FeCO_3$ signals from the in-situ XRD [45]. There is a clear peak in the current transient indicating the formation of crystalline $FeCO_3$ scale. Peak area calculation from the XRD result also indicates $FeCO_3$ formation during the increasing portion of the current transient and then a rapidly decreasing rate of $FeCO_3$ formation as the anodic current decreases towards the end of the test, indicating the growth of a protective surface scale. In this in-situ studies, it was identified that siderite is formed only when the critical super-saturation is exceeded within a defined boundary layer. In

addition this study also indicated that the steel microstructure has a critical role in developing a surface texture within which the state of critical super-saturation can be developed.

In-situ synchrotron X-ray diffraction experiment also revealed the effect microstructure in modulating the morphology of the scale by changing the diffusion conditions on the steel surface and thus affecting the local supersaturation of siderite and forming of surface texture within which the critical supersaturation can be developed. In the recent years Ko et.al. [53] employed in-situ synchrotron X-ray diffraction experiment in order to investigate the effect of microstructure and boundary layer conditions on CO_2 corrosion of low alloy steels. This investigation demonstrated that the nucleation of crystalline scales onto the steel surface at elevated temperature is critically dependent on the initial surface roughness as well as the microstructure-related surface roughness developed during corrosion.

In spite of a significant number of in-situ X-ray diffraction studies, a fundamental question which was not answered was relating to the dependence of the mechanism of nucleation and subsequent growth of crystalline scale leading to a final scale morphology which will be protective or otherwise. This question links to a fundamental question about the precursor state from which crystal nucleates onto the metal surface and the correlation of nucleation with supersaturation under the influence of solution species and other environmental (local or global) conditions. Fundamental challenges to address this interesting question requires proper experimental design and methods wherewith it is possible to control supersaturation and at the same time it allows measurement of the composition precursor, and crystal and their size distribution at different stages of nucleation and growth.

Ingham et al [54] illustrated the subsequent development and gradual growth of siderite crystal from its amorphous state during CO_2 corrosion of plain carbon steel in brine environment. Using *in-situ* synchrotron small- and wide-angle X-ray scattering (SAXS and WAXS) Ingham et al. [54] were able to establish a model with which they explained that the formation of crystalline siderite ($FeCO_3$) during the corrosion of steel in CO_2-saturated brine is actually preceded by the formation of an early stage colloidal precipitate and an amorphous surface layer. GISAXS showed that upon the application of an anodic potential, film forms instantaneously and then a separate population of particles develops in the later stage followed by the formation of the ultimate crystalline $FeCO_3$ as observed by WAXS. Ingham et al. [54] interpreted these observations in terms of crystal nucleation within the amorphous surface layer. This observation suggested to bear a direct consequence on the morphology of the corrosion scale and hence its protectiveness. However, it would perhaps be important to generate an understanding of the effects of changes in local pH and temperature in this gradual formation and development of siderite scale on a more quantitative level.

3. FACTORS INFLUENCING CO_2 CORROSION

CO_2 corrosion and its associated siderite scale formation are strongly influenced by a number of environmental, as well as metallurgical variables [7, 15]. These parametric variables can interact in several ways to influence CO_2 corrosion [7]. There has been an elaborate discussion of the effects of

these parameters in the literature [e.g. 4, 7, 15]. This review therefore simply outlines some of the most important effects.

3.1. Environmental Factors

Solution pH directly influences the corrosion rate by modulating the electrochemical reaction and indirectly influences the precipitation of protective scales. In a solution with a pH less than 7, corrosion rate has been found to be decreased with increasing pH [4, 55]. Change in pH alters the rate of formation of corrosion products/scale by altering the reaction rates at the cathode and anode. For example, increase in pH decreases cathodic reduction of H^+. In addition, pH also affects corrosion film formation and its protectivity by altering the solubility of ferrous carbonate and its subsequent supersaturation. Chokshi et al. [56] found a relatively porous, non-adherent and unprotective layer of siderite at lower supersaturation induced by lower pH (<5).

Kermani et al. [7] provided a "Rule of Thumb" for corrosion rates carbon and low-alloy steels in relation with the pCO_2 which was derived based on field experience and suggested by the American Petroleum Institute, API, in the late 1950s. According to this Thumb-rule, for pCO_2 < 0.5 bar (7 psi) corrosion rate is likely to be <0.1 mm/y, while for pCO_2 > 2 bar (30 psi), corrosion rate could exceed 1 mm/y. In general, higher pCO_2 generally increases the concentration of dissolved carbonic acid species and hence decreases solution pH which in turn enhances the cathodic reaction leading to higher corrosion rates. However, this scenario is true under conditions when the scale cannot form. Bai and Bai [55] demonstrated a detrimental effect (increase in corrosion rate) of increasing CO_2 concentration within a partial pressure range of 3 - 35 bar. However, when other conditions are favorable, higher CO_2 concentration can favor the formation of ferrous carbonate scale. For example, at a higher pH, the higher partial pressure of CO_2 (pCO_2) may lead to an increase in bicarbonate and carbonate ion concentration which in turn enhances supersaturation and accelerates precipitation of a protective scale. Sun and Nesic [57] showed that at pH ≤ 5.2 and temperature ~ 90°C corrosion rates decrease with increase of pCO_2 for both at top and bottom of the pipe in stratified wet gas flow condition.

Temperature accelerates all the sub-processes involved in corrosion including the electrochemical, chemical as well as the transport processes. Therefore, corrosion rate is expected to increase steadily with temperature. However, this is the case only at lower pH, at which a protective scale is not formed. Marked changes in the situations are found when the solubility limit for ferrous carbonate is exceeded (typically in a higher pH range) where increased temperature rapidly accelerates the precipitation kinetics and hence the formation of a protective scale.

Kermani and Smith [15] as well as Waard and Lotz [26] demonstrated how at a particular CO_2 partial pressure corrosion rate initially increases up to a certain temperature and then start decreasing at higher temperatures. The decrease in corrosion rate at higher temperature was attributed to the formation of a protective scale on the steel surface. A maximum in the corrosion rate with increasing temperature is normally (pCO_2 = 1bar) observed within the temperature range of 60 and 80°C depending on water chemistry and flow parameters. Notably however, increasing pCO_2 is capable of

inducing protective scale formation and consequent reduction in the corrosion rate at a lower temperature range and vice versa.

Fluid flow may influence CO_2 corrosion based on whether or not other conditions are conducive to form a protective scale. Typically at low pH (< 4) where the formation of a protective scale is unlikely, the higher flow rate (especially turbulent) would enhance transport of species toward and away from the metal surface leading to an enhanced corrosion rate [4, 55]. On the other hand at higher pH, when protective ferrous carbonate ($FeCO_3$) layers form on the steel surface, the effect of flow becomes insignificant [26]. However, higher flow rates might mechanically affect the scale leading to the risk of localized attack.

The presence of oxygen has a strong influence on corrosion rate, occasionally causing localized attack in a sweet system. Gulbrandsen et al. [59] reported an increase of corrosion rate by ~ 10s mm/year with an increase in oxygen contamination from 1 to 100 ppb in the presence and absence of corrosion inhibitor (CI) at 40°C. At significantly high concentration oxygen was found to impair the performance of CI. Martin [60] reported an increase of corrosion rate in the presence of oxygen by 0.25 to 0.75 mm/year per ppm of oxygen at ambient temperature.

Organic acids (e.g. acetic acid) increase the general corrosion rate, particularly at low pH (≤ 4) and at relatively high temperature (> 60°C).This effect is reduced at higher pH and vanishes at pH 6 or higher [61]. The presence of acetic acid has been found to inhibit the anodic dissolution of iron [61, 62,63] and enhance the cathodic reaction by providing additional hydrogen ions and by direct reduction of free acetic acid on the steel surface. However, Sun et al. [62] reported that the presence of acetic acid increases the cathodic limiting current density only and do not influence the cathodic charge transfer reaction rate significantly, indicating the likelihood of reduction of hydrogen ions to be more likely rather than a direct reduction of acetic acid at the steel surface. Crolet et al. [61] on the other hand suggested that the inhibition effect in the presence of acetic acid is the result of the formation of a corrosion product layer rather than its influence on the cathodic or anodic reactions. Iron acetate can be formed as a result of the replacement of bicarbonate ion with acetate ion and acetate complex can be formed at a relatively higher temperature when the concentration of acetic acid is significantly high [63]. The acetate complexes formed may cause further dissociation of acetic acid leading to lowering of the solution pH and hence causing formation of iron carbonates to be less favorable. Nonetheless, Nafday and Nesic [64] did not notice any significant effect on the iron carbonate scale formation and protectiveness on carbon steel over a range (0-180 ppm) of acetic acid concentrations at 80°C and pH 6.6.

In context of this review, it would be important to address how in-situ synchrotron-based study, in general, can help to formulate a deeper understanding of the effect of various environmental factors on the mechanism of scale formation through stages. The strength of in-situ synchrotron-based study lies in its ability to monitor the real-time changes in the morphology/structure/chemistry of the scale from its precursor stage up until its maturity and its power of resolving the instantaneously formed species even at atomic size level by the proper choice of its operational mode. For example, SAXS can distinguish practice size and distribution over a range of 1-100 nm, GISAXS can identify the nucleation of corrosion scale at the metal surface and the subsequent development of the film at very early stages [54]. Using these powerful techniques it is possible to identify and interpret some

phenomena during the early and intermediate stages of scale formation in terms of local environmental changes (e.g. local changes in pH, temperature, surface property, species concentration, degree of supersaturation etc.) which otherwise would have not been realized or interpreted only in consideration of the global environment mediated thermodynamics.

3.2. Metallurgical variables

In the oil and gas industry, pipelines, wells and processing equipment are mostly made out of CLASs. Unfortunately, in many oil fields CO_2 corrosion of CLAS has been prevalent mainly because of inadequate knowledge of upgrading properties of CLAS. An obvious consequence of this was to choose highly expensive corrosion resistant alloys (CRA) in order to mitigate CO_2 as well as mixed mode CO_2/H_2S corrosion. However, resorting to CLAS with a judiciously tailored property is likely to resolve the problem with a significantly lower cost. In fact, in consideration of the cost of equipment failure due to CO_2 corrosion, the most strategic material of choice by all mean has been suggested to be CLAS [1, 12-17]. However, to be able to tailor the property of the CLAS and making it suitable for specific application would be the key issue.

One of the major areas of research in terms of property upgrade of CLAS has been micro-alloying. Proper choice of micro-alloying elements in combination with appropriate heat treatment and other metallurgical processing render CLAS adequately high corrosion resistance, mechanical performance, weldability, as well as low cost. Amongst the established facts of property improvement by micro-alloying, addition of chromium demonstrated significantly improved corrosion resistance in the CO_2 environment. [19, 58]. Kermani et al [19] as well as Edmonds and Cochrane [12] demonstrated the superiority of CLAS micro-alloyed with 3wt. % Cr for downhole and other oilfield applications. The corrosion performance of CLAS micro-alloyed with 3wt. % Cr showed 3-10 times better corrosion performance with a cost hike of no more than 1.5%. Further addition of micro-constituents (e.g. V, Ti, Si, Mo, and Cu) with 3wt. % Cr micro-alloyed CLAS were found to be beneficial for corrosion performance in CO_2 environment.

Edmonds and Cochrane [12] as well as Kermani et al. [7, 19] used a series of alloy compositions with varying percentage of micro-alloying and indicated the best performing alloy under sweet environment was an alloy with chemical composition (in wt. %) of C: 0.073, Mn: 0.50, Si: 0.31, S < 0.005, P < 0.001, Al: 0.039, V: 0.46, N: 0.011, Mo < 0.02, Cr = 2.81, Cu: 0.50, Fe: balance. The alloy chemistry was designed in a way which can ensure sufficient amount of free chromium (Cr) in solid solution. This criterion was fulfilled by addition of an allowable percentage of transition elements e.g. V, Ti, Mo, Cu etc. which restrict Cr from carbide formation. Kermani et. al. [19] demonstrated the effect of the presence of Cr (in wt. %) in the CLAS on corrosion rate as well as the effects of the presence of other elements on the corrosion rate in the presence of Cr.

Even though the fact of stable, adherent and protective siderite scale formation in the presence of trace amount Cr^{3+} was known [19, 58], the mechanism associated was not clearly understood until in-situ synchrotron SAXS study revealed a clearer picture of the mechanistic aspect of the accelerated siderite film formation in the presence of traces of Cr^{3+} [49,54]. In-situ synchrotron GISAX study

indicated that trace amount of Cr^{3+} in the solution significantly expedites the precipitation rate of the colloidal precursor and thus accelerates the appearance of the crystalline scale. It is assumed that the chromium cation catalyzes the nucleation process by modulating the local pH level at the steel surface and thus reduces the critical supersaturation for precipitation. This study also indicated the interdependence between microstructure and chromium-enhanced siderite nucleation. However, investigating the quantitative effects of surface roughness and other metallurgical factors on the initial nucleation rate of the scale, its subsequent growth rate and protectivity would be a good addition to this study.

4. CONCLUDING REMARKS

Conventional ex-situ methodologies and analyses have been extensively employed to study CO_2 corrosion of oil pipelines and gas wells. These studies were helpful to analyze the end corrosion product and hence only could reveal how the protectiveness of the final scale can be related to the end chemistry, the morphology of the scale. However, only a little information was available on the experimental as well as theoretical analyses of the anodic reactions that directly relates to the formation of carbonate scale. In addition, the information available on the early nucleation stages of scale formation was also very limited and the mechanism of early stage nucleation and subsequent growth of an adherent and protective siderite layer were ambiguous. Recent investigations and analyses using powerful in-situ synchrotron techniques, e.g. SAXS, GISAXS, WAXS provided promising information towards a deeper understanding of the mechanism of the early stage nucleation and subsequent growth of the siderite crystal by enabling the monitoring of real-time growth of surface layers on the steel surface. With the use of SAXS and in particular GI-SAXS, it has been indicated that the formation of siderite crystal is preceded by the formation of colloidal precipitate in the solution and a thin gel surface layer. The use of WAXS on the other hand indicated the formation of cluster of particles within that thin gel surface layer which has been assumed to be the amorphous ferrous carbonate.

Another aspect is the choice of proper materials in order to achieve the lowest possible cost to durability ratio. In consideration of the cost to durability ratio, the most strategic material of choice has been shown to be CLAS with properly tailored properties. The application specific desired properties can be achieved by formulating the chemistry of the steel by incorporating appropriate alloying elements and by modifying the microstructure through proper heat treatment. Effect of micro-alloying with number of elements in various proportions has been studied. For example, the effect of improvement in corrosion resistance by the presence of low level chromium was attributed to the formation of a 'more protective' chromium rich scale. However, no mechanistic detail of how the presence of chromium is enhancing scale protectivity is yet unclear. GI-SAXS in the recent time indicated the instantaneous film formation on the metal surface in presence Cr^{3+} upon the application of an anodic potential. This was indicated to be the Cr^{3+} induced accelerated precipitation of colloidal precursor as well as the accelerated rate of formation of subsequent crystalline siderite scale which can be a plausible interpretation for the steel to acquire better corrosion resistant in the presence of trace

amounts of Cr. More detailed and qualitative information is yet required in order to understand how Cr and other alloying elements modulate the mechanism of the early stage nucleation and subsequent growth protective scale under various environmental conditions. Combined ex-situ electrochemical study and in-situ synchrotron-based electrochemical experimentation is likely to be the effective tool.

References

1. M B Kermani, J Martin, K Esaklul, *Corrosion, NACE International* (2006), paper 6121.
2. S. N. Smith, M W. Joosten, *Corrosion, NACE International* (2006), paper 6115.
3. Y S Choi, S Nesic, S Ling, *Electrochimica Acta,* 56 (2011) pp. 1752.
4. S. Nesic, W. Sun, "Corrosion in Acid Gas Solutions", *Shreir's Corrosion,* 2 (2010) 1270.
5. S. N. Smith, M W. Joosten, *Corrosion, NACE International,* (2015) paper 5484.
6. M. Bonis, R Mcdonald, *Corrosion, NACE International,* (2015) paper 5718.
7. M. B. Kermani , A. Morshed, *Corrosion*, 59 (2003) 659.
8. A. Traidia, M. Alfano, G. Lubineau, S. Duval, A. Sherik, *Int. J. Hydrogen Energ.* 37 (2012) 16214.
9. M.A. Lucio-Garcia, J. G. Gonzalez-Rodriguez, M. Casales, L. Martinez, J. G. Chacon-Nava, M. A. Neri-Flores, *Corrosion. Scence.*, 51(2009) 2380.
10. M. Al-Mansour, A. M. Alfantazi, M. El-Boujdaini, *Mater. & Design,* 30 (2009) 4088.
11. E. Ramíreza, J.G. González-Rodrigueza, A. Torres-Islasa, S. Sernaa, B. Campillob, G. Dominguez-Patiñoa, J.A. Juárez-Islasc, *Corros. Sci.*, 50 (2008) 3534.
12. D. V. Edmonds, R C. Cochrane, *Materials Res.*, 8 (2005) 377.
13. D. E. Cross, *Corrosion, NACE International,* (1993), Paper 118.
14. J. L. Crolet. In 'Predicting CO$_2$ Corrosion in the Oil and Gas Industry'. M. B. Kermani and L. M. Smith, editors, *EFC (European Federation of Corrosion)*, 1994.
15. M.B. Kermani, L. M. Smith. 'CO$_2$ Corrosion Control in Oil and Gas Production – Design Considerations'. *EFC (European Federation of Corrosion)*; London: IoM, 1999.
16. V. Rabald. 'Corrosion Guide', 2nd ed, Elsevier, Amsterdam, Nethderland, (1968) 76.
17. ASM Metals Handbook. *'Corrosion'.* vol. 13, 1987.
18. G. E. King, Corrosion Overview, 2014 [cited 2014 1 June]; Available from: http://gekengineering.com/
19. M. B. Kermani, J. C. Gonzales, G. L. Turconi, D. Emonds, G. Dicken, L. Scoppio, *Corrosion, NACE International* (2003) paper 3116.
20. T. Li, Y. Yang, K. Gao, M. Lu, *J. Univ. Sci. Technol - Beijing,* 15(2008) 702.
21. R. Nyborg, *Corrosion, NACE International* (2002), paper 02233.
22. R. Bonis and J. L. Crolet, *Corrosion, NACE International* (1989) paper 46619.
23. K. Videm, *Proceedings from 10th European Corrosion*, *Progress in the Understanding and Prevention of Corrosion*, *Vol.1*, Institute of Metals, London, 1993, paper 513.
24. P.A. Burke, *Corrosion, NACE International*, (1984) paper 3.

25. G. Schmitt, *Corrosion, NACE International*, (1984) paper 10.
26. C. Waard and U. Lotz, *Corrosion, NACE International* (1993) paper 69.
27. A. Ikeda, M. Ueda, and S. Mukai, *Corrosion, NACE International* (1983) paper 45.
28. J. L. Crolet, *Proceedings from 10th European Corrosion*, *Progress in the Understanding and Prevention of Corrosion*, , Institute of Materials, London, *Vol.1* (1994) paper 1.
29. C. A. Palacios and J. R. Shadley, *Corrosion* 47(1991) pp.122.
30. J. L. Crolet, N. Heverot, S. Nesic, *Corrosion, NACE International* (1996) paper 4.
31. A. Dugstad, *Corrosion, NACE International*, (1998) paper 31.
32. Y S Choi, S Nesic, D Young, *Environmental science & technology,* 44 (2010) 9233.
33. I. Rippon, *Corrosion, NACE International* (2001) paper 1055.
34. B. F. M. Pots, R. C. John, I. J. Rippon, M. J. J. S. Thomas, S. D. Kapusta, M. M. Girgis, T. Whitham, *Corrosion, NACE International* (2002) Paper 2235.
35. Philip L Fosbol in CO_2 Corroion: Modelling and Experimental Work Applied to Natural Gas Pipelines, Ph.D. Thesis, Denmark Teknical University, 2008, pp. 58-67.
36. R. Nyborg, *Corrosion, NACE International*, (2010), Paper 10371.
37. S Nesic and L.Lunde, *Corrosion*, 50 (1994) 717.
38. G Lin, M Zheng, Z. Bai, and Y. Feng, *J. Iron Steel Res. Int*. 13 (2006) 47.
39. F. Yu , K. Gao, Y. Su, J. Li, L.Qiao, W. Chu, and M. Lu, *Mater. Lett*. 59 (2005) 1709.
40. J. Han, D. Young, H. Colijn, A. Tripathi, and S. Nesic, *Ind. Eng. Chem. Res.*, 48 (2009) 6296.
41. De Marco, R., Jiang, Z.-T., Pejcic, B. and Poinen, E., *J. Electrochem. Soc.*, vol. 152. pp. B389-92.
42. C. D. Waard and D. E. Milliams, *Corrosion*, 31(1975) 177.
43. S. Nesic, J. Postlethwaite and S. Olsen, *Corrosion*, 52 (1996), 280.
44. L. G. S. Gray, B. G. Anderson, M. J. Danysh and P. R. Tremaine, *CORROSION, NACE International,* (1989), Paper 464.
45. B. Ingham, M. Ko, G. Kear, P. Kappen, N. Laycock, J. A. Kimpton and D. E. Williams, *Corros. Sci.*, 52 (2010) 3052.
46. M Ko, B Ingham, N Laycock, D E Williams, *15th Middle East Corrosion Conference and Exhibition*, (2014) paper 14189.
47. M. R. Bonis and J. L. Crolet, *Corrosion, NACE International,* (2005), Paper 05272.
48. J. L. Crolet, S. Olsen and W. Wilhelmsen, *Corrosion, NACE International* (1995) Paper 127 and J. L. Crolet, in "Modelling Aqueous Corrosion From Individual Pits to System Management", ed. K. R. Trethewey and P R Roberge, *NATO ASI Series, Series E: Applied Sciences,* 1994, vol. 266, pp 1-28.
49. M. Ko, B. Ingham, N. Laycock, D. E. Williams, *Corros. Sci.*, 80 (2014) 237.
50. B. Ingham, M. Ko. N. Laycock, J. Burnell, P. Kappen, J. A. Kimpton and D. E. Williams, *Corros. Sci*, 56 (2012) 96.
51. M. Ko, B. Ingham, N. Laycock and D. E. Williams, *Corros. Sci*, 68 (2012) 1085.
52. M. Ko, B. Ingham, N. Laycock, J. Burnell and D. E. Williams, *proceeding of ACA Conference*, 2012, Melbourne, Australia.
53. M. Ko, B. Ingham, N. Laycock, D.E. Williams, *Corros. Sci.*, 90 (2015), 192.
54. B. Ingham, M. Ko, N. Laycock, M. M. Kirby and D. E. Williams, *Faraday Discuss.*, 180 (2015) 171.
55. Y. Bai and Q. Bai, Subsea Pipeline Integrity and Risk Management, 1st ed., Elsevier, Amsterdam, (2014) pp. 3-25.
56. K. Chokshi, W. Sun, S. Nesic, *Corrosion, NACE International* (2005) Paper 285.
57. Y. Sun, S. Nesic, *Corrosion, NACE International* (2004) paper 4380.
58. M. Ueda, H Takabe, *Corrosion, NACE International* (2002) paper 2041.
59. E. Gulbrandsen, J. Kvarekval, and H, Miland. *Corrosion*, 61(2005) 1086.
60. R. L. Martin, *Corrosion, NACE International* (2002) paper 270.
61. J. L. Crolet, N.Thevenot and A. Dugstad, *Corrosion, NACE International* (1999) paper 24.

62. Y. Sun, K. George and S. Nesic, *Corrosion, NACE International* (2003) paper 3327.
63. J. Amri, E. Gulbrandsen, R.P. Nogueira, *Corros. Sci.*, 52 (2010) pp. *1728*.
64. S. Nesic, *Corros. Sci.*49 (2007) pp. 4308.